Published in final edited form as:
J Cell Sci Ther. 2014 January 30; 5(1): 153–. doi:10.4172/2157-7013.1000153.

Cardiomyocyte-specific Estrogen Receptor Alpha Increases Angiogenesis, Lymphangiogenesis and Reduces Fibrosis in the Female Mouse Heart Post-Myocardial Infarction

Shokoufeh Mahmoodzadeh[#1,*], **Joachim Leber**[#1], **Xiang Zhang**[#1,2], **Frédéric Jaisser**[3], **Smail Messaoudi**[3], **Ingo Morano**[4], **Priscilla A Furth**[5], **Elke Dworatzek**[1], and **Vera Regitz-Zagrosek**[1]

[1]Institute of Gender in Medicine and Center for Cardiovascular Research, Charité Universitaetsmedizin, Berlin, Germany

[2]Department of Cardiology, The Fourth Affiliated Hospital of Harbin Medical University, Harbin, China

[3]Inserm, U872, Paris, France

[4]Max-Delbrueck-Center for Molecular Medicine, Berlin, Germany

[5]Departments of Oncology and Medicine and the Lombardi Comprehensive Cancer Center, Georgetown University, Washington, DC, USA

[#] These authors contributed equally to this work.

Abstract

Experimental studies showed that 17β-estradiol (E2) and activated Estrogen Receptors (ER) protect the heart from ischemic injury. However, the underlying molecular mechanisms are not well understood. To investigate the role of ER-alpha (ERα) in cardiomyocytes in the setting of myocardial ischemia, we generated transgenic mice with cardiomyocyte-specific overexpression of ERα (ERα-OE) and subjected them to Myocardial Infarction (MI). At the basal level, female and male ERα-OE mice showed increased Left Ventricular (LV) mass, LV volume and cardiomyocyte length. Two weeks after MI, LV volume was significantly increased and LV wall thickness decreased in female and male WT-mice and male ERα-OE, but not in female ERα-OE mice. ERα-OE enhanced expression of angiogenesis and lymphangiogenesis markers (*Vegf, Lyve*-1), and neovascularization in the peri-infarct area in both sexes. However, attenuated level of fibrosis and higher phosphorylation of JNK signaling pathway could be detected only in female ERα-OE after MI. In conclusion, our study indicates that ERα protects female mouse cardiomyocytes from the sequelae of ischemia through induction of neovascularization in a paracrine fashion and impaired fibrosis, which together may contribute to the attenuation of cardiac remodelling.

[*]**Corresponding author:** Shokoufeh Mahmoodzadeh, Institute of Gender in Medicine, Center for Cardiovascular Research, Hessische Str. 3-4, 10115 Berlin, Germany, Tel: +49 (0)30 450 525 287; Fax: +49 (0)30 450 525 943; s.mahmoodzadeh@charite.de.

Keywords

Estrogen receptor alpha; Myocardial infarction; Angiogenesis; Lymphangiogenesis; Cardiac fibrosis

Introduction

The incidence of Cardiovascular Diseases (CVD) and its associated mortality is lower in premenopausal women compared to aged-matched men, but increases rapidly after menopause and reaches similar level as in men (for review see [1]). These data suggest that 17β-estradiol (estrogen, E2) prevents CVD in premenopausal women and contributes to the observed sex differences. Accordingly, several clinical studies and experimental animal settings showed that E2 deficiency has been associated with an increased risk of mortality after cardiac injury, which was improved by E2 supplementation [2-4]. Experimentally, administration of E2 reduced infarct size and cardiomyocyte apoptosis [5-7], improved myocardial recovery and viability after Ischemia-Reperfusion (I/R) injury in different animal models [8-14]. The treatment with Estrogen Receptor (ER) antagonist ICI 182 780 reversed the E2-induced effects indicating that these effects are mediated by ER [8]. However, E2 and its receptor effects on the heart and vasculature are incompletely understood, and require a better basic understanding of the underlying mechanisms.

ER-alpha (ERα) is one of the known ER which mediates, at least partly, the beneficial effects of E2 on the heart during stress, in a genomic or non-genomic manner [15]. ERα is expressed and localized in different cardiac cell types of humans and rodents, such as cardiomyocytes, fibroblasts and endothelial cells [16-20]. Increased expression of ERα could be detected in the heart of patients with aortic stenosis and dilated cardiomyopathy, most likely as a compensatory mechanism [18,19]. The absence of ERα is associated with the increased presence of atherosclerotic plaque in humans, especially in premenopausal women [21,22]. In line with these findings, it has been demonstrated that ERα-knockout (ERKO) mouse hearts subjected to I/R had fewer viable cardiomyocytes, decreased coronary flow rate, marked myocardial edema, more prominent mitochondria damage, and decreased functional recovery of contractility and compliance compared with WT-mice [23,24]. By contrast, administration of an ERα-selective agonist during Myocardial Infarction (MI) and the following phenomenon of I/R injury results in the reduction of infarct size, neutrophil infiltration, oxidant stress, necrosis, and improvement of myocardial recovery [9,10,25-27]. These data suggest that ERα contributes to myocardial salvage after injury, and it is of critical importance to understand the relative role of this receptor in the heart. However, the activity of ERα is tightly regulated in a cell specific manner through complex processes which are still not fully understood. Since cardiomyocytes are more susceptible to ischemia than other cardiac cell types and their survival determines the outcome after myocardial ischemia [28], we aimed to analyze the specific role of ERα in cardiomyocytes during ischemia. We therefore generated a transgenic mouse model with a cardiomyocyte-specific ERα overexpression (ERα-OE) and subjected mice of both sexes to MI. We chose a gain of function approach, since it allows us to study the *in vivo* potential role of activation of ERα in cardiomyocytes, which is not feasible in a loss of function

approach. This study helps to elucidate the protective potential of ERα in cardiomyocytes under ischemic conditions. Targeted activation of ERα to enhance cardioprotective mechanisms could provide novel therapeutic options for the diseased hearts.

Materials and Methods

Transgenic animals

Inducible double transgenic mice with cardiomyocyte-specific ERα overexpression (ERα-OE) were generated through mating of monotransgenic ERα (tetO-mERα) and monotransgenic α-MHC-tTA mice using Tet-Off system (for more details see Material and Methods in the supplementary material). Since cardiac phenotype and function of monotransgenic tetO-mERα and α-MHC-tTA mice did not significantly differ from wild type-littermates (WT, data not shown), we did not include the monotransgenic mice in further analysis, and only the WT-littermates were used as control. All animal experiments were approved by and conducted in accordance with the guidelines set out by the State Agency for Health and Social Affairs (LaGeSo, Berlin, Germany, G 0360/08) and conform to the Guide for the Care and Use of Laboratory Animals published by the US National Institutes of health (NIH Publication No. 85-23, revised 1996).

Myocardial infarction model

MI was induced in Female (F) and Male (M) mice at 12 weeks of age, by permanent left anterior descending Coronary Artery (LAD) ligation. Mice were anesthetized with ketamine hydrochloride (80 mg/ml)/xylazine hydrochloride (12 mg/ml) solution administered by intraperitoneal injection at a dose of 1 mg/kg. Briefly, after intubation, LAD coronary artery was ligated with a 7.0 polypropylene suture. As non-infarcted controls, mice underwent a sham operation where the ligature around the LAD was not tied. Animals were recovered from anaesthesia under warming conditions and normal ventilation. The animals were treated with rimadyl (5 mg/kg) for analgesia up to 7 days post-surgery. Two weeks after MI, animals were sacrificed and hearts were harvested for further analysis. To evaluate cardiac function and morphology, echocardiography was performed before thoracotomy, and 14 days after MI in sedated mice with the echocardiography system (Vevo 770 High-Resolution Imaging System, Toronto, Canada) equipped with a 20-55 MHz transducer.

Infarct size was determined as described somewhere else [29]. Briefly, two-dimensional cineloops from the parasternal long axis view were acquired using the EKV™-mode (ECG-Gated Kilohertz Visualization), which allows the assessment of cardiac wall motion with the highest temporal resolution available in small animal imaging today (≡1000 frames per second). For MI size determination, the full cardiac cycle was displayed in slow motion in order to clearly identify infarcted zones, which were thinned and akinetic. The internal border of the infarcted zone (MI border) and the endocardial border of the whole LV (LV border) were traced at end-diastole. MI size (in %) was calculated as: MI border × 100/LV border.

Isolation of adult mouse ventricular cardiomyocytes and cell culture

Ventricular cardiomyocytes were isolated from 2-3 month old female and male WT- and ERα-OE mice by a standard enzymatic technique as described before [30]. Briefly, animals were anesthetized with isoflurane, followed by intraperitoneal injection of 8 μg xylazine and 35 μg ketamine. Hearts were rapidly removed and perfused with a low Ca^{2+}, collagenease bicarbonate buffer solution (36°C, pH 7.4) for 10 min. Subsequently, the ventricles were minced. After several wash steps, isolated cardiomyocytes were finally resuspended in M199 medium (Sigma, Germany) supplemented with 0.2% bovine serum albumin, 5% fetal calf serum, 5 mmol/l creatine, 5 mmol/l taurine, 2 mmol/l carnitine, 10 μmol/l cytosine-D-arabinofuranoside, and antibiotics. Cardiomyocytes were seeded in with 0.2% laminin-coated 4-well chamber slides (Nunc, Wiesbaden-Schierstein, Germany) and cultured for 4 h in M199 medium before measurement of their length and width.

Cell morphology

The individual length and width of the cardiomyocytes were determined on micrographs captured by Axiovert 40 CFL microscope (using objective: N-Achroplan 10x/0.25 Ph1 W 0.8) and digitalized by AcioCam MR3 camera. Ten micrographs per sample were randomly taken, and 100 to 300 rod-shaped myocytes were measured per sex and genotype. Length and width of cardiomyocytes were determined at the widest point of each myocyte using the software program “AxioVision Release 4.8” (Zeiss).

Gene expression analysis

Total RNA isolation and quantitative Real-Time Polymerase Chain Reaction (qRT-PCR) was conducted as previously described [31]. Quantification of expression levels of the mouse ERα (*Esr1*), atrial natriuretic peptide (*Nppa*), brain natriuretic peptide (*Nppb*), myosin heavy chain 6 and 7 (*Myh6*, *Myh7*), platelet/endothelial cell adhesion molecule-1 (Pecam-1 or *CD-31*), vascular endothelial growth factor (*Vegf*), lymphatic vessel endothelial hyaluronan receptor-1 (*Lyve-1*), collagen type I and III (*Col I* and *Col III*) was performed by real time PCR, using SYBRGreen (Bio-Rad Laboratories, Hercules, CA, USA). The housekeeping gene Hypoxanthine Phosphoribosyltransferase (*Hprt*) was used to normalize the results. Primer sequences used for amplification are listed in (Table S1).

Western blot analysis

Western blot analyses were performed using whole LV tissues isolated from female and male ERα-OE mice ($n \geq 8$) or WT-mice ($n \geq 8$) as previously described [19]. Briefly, for each sample, 25 μg of protein was loaded into a 10% polyacrylamide gel, electrophoresed, and transferred to a nitrocellulose membrane. Western blot analyses were performed using a standard protocol with specific primary antibodies against ERα (G-20, Santa Cruz), phospho-ERα (pERα (serin 118)-R; Santa Cruz), mitogen-activated protein kinase c-jun N-terminal kinase JNK1/3 (C-17, Santa Cruz), p-JNK (G-7, Santa Cruz), GAPDH (clone 6C5, Millipore) and donkey anti-mouse IgG or donkey anti-rabbit IgG secondary antibody (Jackson Immuno Research Laboratories). Specific bands were visualized using ECL™ detection kit (GE Healthcare). Band intensities were quantified with ImageJ software 1.37V.

Histological analysis

After dissection, the transverse midsection of the LV was immediately fixed in 4% formaldehyde for 24 h and paraffin-embedded for sectioning. Serial tissue sections (3 μm) were cut and routinely stained with Hematoxylin-Eosin (H&E) and visualized by light microscopy. To analyze the changes in fibrotic areas, LV sections were stained with Sirius red to determine collagen deposition. The fibrosis area was measured and calculated as the percent of the area of fibrosis to entire cross-sectional area of LV by using the Media Cybernetics Image Pro PLUS software (Bethesda, MD).

Immunofluorescence analysis

Double-labeling immunofluorescence histochemistry was performed as previously described [18]. Briefly, after paraffin-embedded LV sections (3 μm) were deparaffinized with Neoclear (Merck, Germany) and rehydrated to PBS, the sections were subjected to heat-mediated antigen retrieval by pressure cooking in 10 mM citric acid buffer, pH 6.0. After cooling down to room temperature for 20 min, and 1 h of blocking in 1%BSA-PBST (1×PBS+0.2% Tween) at room temperature, sections were incubated with primary antibodies against CD31 or PECAM-1 ((M-20) SC-1506-R, 1:200 dilution) and against LYVE-1 ((Xb-13) SC-80170, 1:50 dilution) overnight at 4°C. After washing, sections were incubated with secondary FITC-conjugated anti-rabbit IgG (Jackson ImmunoResearch Laboratories) and Cy3-conjugated anti-rat IgG (Jackson ImmunoResearch Laboratories) both at a dilution of 1:100 in 0.1% BSA-PBST for 1 h at RT. Nuclei were stained with 6-diamidino-2-phenylindole (DAPI). Finally, sections were mounted with VectaShield H-1000 (Linaris) and viewed on an upright fluorescence microscope (Olympus BX61). Negative controls included sections in which either the primary antibody or secondary antibody or both were omitted. In these sections no signals for CD31 and LYVE-1 were detectable. Quantification of immunoreactivity by pixel intensity was analyzed by Image Pro PLUS software (Bethesda, MD). The ratio of area of CD31 or LYVE-1 expressing vessels to whole LV cross-sectional area was calculated.

For detection of ERα in the LV sections of WT and ERα-OE mice, following antibodies were used: primary antibody anti-ERα (G20, Santa Cruz), secondary antibody FITC conjugated goat anti-rabbit (Jackson laboratory). Confocal images were acquired using a Leica TCS-SPE spectral laser scanning microscope, and images were processed by Leica Application Suite AF software (version 1.8.0).

Statistics

All data are presented as mean ± standard error of the means (SEM). Statistical analysis was performed using One-way ANOVA followed by Bonferroni's test to compare multiple groups, and two-tailed Student's t-test to compare the mean of two groups. Kaplan–Meier curves were created to illustrate cumulative mortality after MI, and statistical assessment was performed by the log-rank test. Statistical analyses were performed using software Graphpad Prism 5.01. Differences with $p \leq 0.05$ were considered significant.

Results

Characterization of cardiomyocyte-specific ERα overexpressing transgenic mice

We first evaluated the phenotype of a transgenic mouse model with a constitutive cardiomyocyte-specific overexpression of ERα (ERα-OE). Overexpression of ERα was detected in the LV tissues of ERα-OE mice compared to WT-mice using Western Blotting and immunohistochemistry (Figure 1). We found a 10-13 fold increase in the expression of ERα transgene 66 kDa isoform in LV-tissues of female and male ERα-OE mice (Figure 1A). No sex-differences in ERα expression levels were detected. Comparison of ERα expression levels in the LV, kidney, liver, uterus and lung of 12 week-old ERα-OE mice showed that the ERα overexpression was restricted to the heart (Figure 1B). ERα-OE hearts showed a significant increase (3.5-5.0 fold) in the phosphorylation level of ERα compared to WT-mice without sex-differences (Figure 1C). Immunofluorescence data demonstrated a more intense ERα signal in the LV of ERα-OE mice with the strongest signal in the nuclei of cardiomyocytes (Figure 1D).

ERα-overexpression promotes cardiac hypertrophy in the basal state in both sexes

Ratio of LV mass to tibia length (LVM/TL) was significantly increased in ERα-OE compared to WT-mice in both sexes, demonstrating the development of Myocardial Hypertrophy (MH) in ERα-OE mice (table 1). This was due to an increase in ventricular diastolic and systolic volumes, but not wall thickness in both sexes (table 1). On microscopic examination of isolated cardiomyocytes, female and male ERα-OE displayed a significant increase in cardiomyocyte length, but not in cardiomyocyte width compared with WT-mice (Figures 2A-2C). In line with these data, expression of hypertrophic marker genes atrial natriuretic peptide (*Nppa*) and brain natriuretic peptide (*Nppb*) was significantly increased in the LV of ERα-OE mice (Figures 2D and 2E). The ratio of myosin heavy chain 7 and 6 (*Myh7*/*Myh6*) was shifted towards higher expression of the slower *Myh7* isoform (Figure 2F). These findings overall indicate that cardiomyocyte-specific ERα-OE leads to the spontaneous development of cardiac hypertrophy in both sexes.

Survival Analysis after myocardial infarction

To investigate the *in-vivo* potential of ERα overexpression under pathological conditions, MI was induced. The mortality was high within the first 24 h after MI among all groups without significant differences between groups. However, after this acute phase, females ERα-OE survived 100%, suggesting that ERα overexpression in female hearts increased survival after MI, which was not observed in males (Figure 3). Infarct size was similar in both sexes after MI (Table 1). In mice overexpressing ERα, infarct size was slightly decreased compared to WT mice (Table 1) however the difference was not statistically significant.

ERα improves myocardial adaptation after myocardial infarction in females

Similar to female and male WT-mice, male ERα-OE mice showed significant increase in LV volumes and decrease in wall thickness two weeks after MI. In contrast, female ERα-OE hearts showed no significant changes in these parameters (Table 1). Cardiac functional

parameters, such as stroke volume, cardiac output and heart rate, were not significantly different between the groups (Table 1). Although both female and male ERα-OE mice hearts displayed higher expression of molecular MH-indicators (*Nppa* and *Nppb*) at the basal level, MI did not lead to the further increase in the expression of these genes, as observed in WT-mice (Figures 2B and 2C). The hearts of WT-mice of both sexes exhibited a significant increase of *Myh7*/*Myh6* ratio after MI, which was abolished in female and male ERα-OE mice hearts (Figure 2D).

ERα enhances cardiac angiogenesis and lymphangiogenesis after myocardial infarction in both sexes

In paraffin-embedded, Hematoxylin-Eosin-stained (H&E) heart sections from female and male ERα-OE mice, we observed increased occurrence of vascular-like structures predominantly in the peri-infarct area. This was found to a lesser extent in the WT-mice of both sexes (Figures 4A and 4B). To assess the nature of these vessel-like structures, we performed immunofluorescence double staining experiments using antibodies against CD-31 (PECAM-1 or) for the staining of blood vessel, and against LYVE-1 for the staining of lymphatic vessels. Very few CD31 and LYVE-1 positive signals were found in the hearts of WT and ERα-OE sham mice (Figures 4C, 4D, 4G and 4H). After MI, predominately in the peri-infarct areas and to the lesser extent in the infarct areas, the signals for CD31 and LYVE-1 were significantly increased in both female and male ERα-OE mice hearts compared to their respective sham-operated and to WT controls (Figures 4E, 4F, 4G and 4H). Additionally, areas of CD31- and LYVE-1 expressing vessels were significantly greater in both female and male ERα-OE mice hearts than those in WT-mice hearts after MI (Figures 4E-4H). Consistently, the expression of *Vegf*, a key inducer of angiogenesis, and *Lyve-1* were significantly increased in tissues obtained from the infarct and peri-infarct area of female and male ERα-OE mice hearts compared with WT-mice (Figures 4I and 4J). Taken together, ERα-overexpression in cardiomyocytes accelerates both angiogenesis and lymphangiogenesis predominantly in the peri-infarct and infarct areas in both sexes.

ERα induces the phosphorylation of JNK signaling pathway only in female hearts after myocardial infarction

JNK1/3 is known as a positive regulator of angiogenic process [32,33]. Western blot analysis of LV extracts from both female and male WT- and ERα-OE mice showed that the phosphorylation level of JNK was significantly increased only in female ERα-OE mice hearts after MI (Figure 5).

ERα attenuates collagen deposition after myocardial infarction only in female hearts

We next determined the effects of ERα overexpression on *Col* I and *Col* III gene expression and Col deposition in the hearts of ERα-OE and WT-mice after MI. Expression of *Col* I and III were significantly increased in the hearts of both female and male WT-mice after MI, but not changed in ERα-OE mice (Figures 6A and 6B). Of note, female mice with ERα-OE expressed significant less C*ol* I and III than female WT-mice after MI. Collagen staining of mid-LV sections from female and male WT- and ERα-OE mice showed significant increase of collagen deposition in all animals (Figure 6C). However, in line with the diminished *Col* I

and III expression, hearts of female ERα-OE mice showed significantly less collagen deposition after MI, compared with female WT-mice (Figure 6C). Overall, ERα overexpression is associated with less fibrosis in female hearts, suggesting that the female hearts are less susceptible to MI-induced remodelling.

Discussion

In this study, we present novel insights into mechanisms that account for the ERα-dependent myocardial protection against myocardial injury, with more beneficial effects in female hearts. Using transgenic mice with a cardiomyocyte-specific ERα overexpression, we first demonstrated that this was associated with an increase of LVM consistent with the increase of cardiomyocyte length at the basal level in both female and male mice. After MI, the cardiomyocyte-specific ERα-OE inhibited changes in LV-volumes and wall thickness only in female mice. These beneficial effects in female ERα-OE hearts were associated with increased angiogenesis and lymphangiogenesis, attenuated ventricular fibrosis and enhanced JNK phosphorylation. Our study indicates that in the female sex, ERα in cardiomyocytes may have a therapeutic potential in the treatment of ischemic heart disease, leading to more efficient cardiac repair after ischemic injury.

Effects of ERα overexpression on the heart

To address the effect of ERα more precisely on cardiomyocyte following cardiac injury, we generated mice with a constitutive overexpression of ERα in cardiomyocytes. This unique model allows obtaining new insights into ERα mediated Cardioprotective mechanisms. The constitutive cardiomyocyte-specific ERα overexpression resulted in myocardial hypertrophy, associated with higher LVM, increased ventricular volumes, greater cardiomyocyte length, no fibrosis and augmented expression of hypertrophy-associated genes *Nppa* and *Nppb* and *Myh*7/*Mhy*6 ratio in both sexes at basal level. These are characteristics of an eccentric type of physiological hypertrophy, and have been observed in hearts during pregnancy or in the athlete hearts after endurance training [34-37]. The observed effects in our study may be due to direct effects of ERα as a transcription factor through the regulation of expression of hypertrophy-target genes, or indirect due to hemodynamic alterations. We demonstrated in this study a higher phosphorylation of ERα at Ser118, essential for transcriptional activation [38], as well as a greater translocation of ERα in the nuclei of ERα-OE mice cardiomyocytes, pointing to the functional role of ERα as a transcription factor in this model. Additionally, in a previous study we showed that the expression of hypertrophy-associated genes *Nppa*, α-actinin and *Cx43* are increased by E2-induced activation of ERα in a human cardiomyocyte-like cell line AC16 cells [39]. Therefore, the higher expression and activation of ERα could be an explanation for the increased expression of hypertrophy-associated genes in ERα-OE mice. It is also conceivable that the higher expression of *Nppa*, *Nppb* and *Myh*7 in the LV of ERα-OE is in response to increased cardiomyocyte stretch due to increased cardiomyocyte length, as reported elsewhere [40-43].

Effects of ERα overexpression following myocardial infarction

Following MI, hearts of female ERα-OE mice did not exhibit accelerated post-infarct remodelling. Compared to WT and male ERα-OE mice, in female ERα-OE hearts systolic and diastolic volumes were not increased and LV wall thickness not significantly decreased after MI. These phenomena may lead to reduced wall stress in female ERα-OE hearts after MI, thus attenuating the adverse consequences of remodelling.

With this study, we also provide evidence that cardiomyocyte specific ERα overexpression facilitates angiogenesis and lymphangiogenesis (new blood and lymphatic vessels sprouting from pre-existing vessels) in the heart in response to MI in both sexes. In this respect, the mRNA expression of angiogenesis and lymphangiogenesis markers *Vegf* and *Lyve-1*, and the area of both CD31- and LYVE-1 expressing vessels were significantly increased predominately in the peri-infarct and to lesser extent in the infarct area of the hearts from ERα-OE mice. This indicates that ERα induces angiogenesis and lymphangiogenesis in the heart after MI. Our data are in accordance with other studies which provide evidence that the known pro-angiogenic properties of E2 [44-48] are mainly mediated by ERα in different tissues under normal and pathologic conditions. Angiogenesis is impaired in ERKO mice [49-52] or upon ER antagonist-treatment [53] and is increased by ERα-agonist [54]. An important molecule that controls angiogenesis and lymphangiogenesis in the healing area after MI is VEGF [55-57], which can be regulated by E2 in different organs, including the myocardium [44,47,58,59]. It has been speculated that this estrogenic effect is most probably mediated through activation of ERα, since the absence or deficiency of functional ERα leads to the reduction of expression level of *Vegf* and reduced coronary capillary density in female mouse hearts [60,61]. Additionally, it has been reported that E2-activated ER inhibits the expression and secretion of Thrombospondin-1, a negative regulator of angiogenesis, in human umbilical vein endothelial cells through activation of JNK in a non-genomic manner [62]. In line with this data we observed an increased phosphorylation of JNK (pJNK) only in the hearts of female ERα-OE mice after MI. Therefore, we assume that a higher baseline of endogenous E2 in females, compared to males, led to preferential activation of JNK in female ERα-OE cardiomyocytes. The E2/ERα mediated JNK-activation in this study could be either mediated by increased expression of cardiomyocytes-derived VEGF in a paracrine manner, as shown in vascular endothelial cells [32,33], or demonstrates an additional mechanism independent of VEGF in female ERα-OE mice heart.

So far, it is not clear to what extent ERα affects the lymphangiogenesis in the heart after MI. To the best of our knowledge, this study is the first work that shows the involvement of ERα in the enhancement of lymphangiogenesis after MI.

Both angiogenesis and lymphangiogenesis are of clinical interest because of their important roles in wound healing and tissue repair. Angiogenesis advances delivery of both oxygen and energy substrates in peri-infarct and infarct area, and has the potential to salvage ischemic myocardium at early stages after MI [63]. Lymphangiogenesis in the peri-infarct area improves cardiac lymph flow leading to reduced lymphedema, thereby reducing a trigger for the development of interstitial fibrosis [64-66]. Davis et al. [67] demonstrated in a rat model that chronic myocardial edema was accompanied by increased mRNA levels of

Col I and III followed by significant increases in LV collagen deposition. In our study, although both female and male ERα-OE mice displayed increased angiogenesis and lymphangiogenesis, only female ERα-OE mice exhibited significantly reduced expression of *Col* I and III mRNA and less cardiac fibrosis after MI. These data are further supported by our recent study showing that ERα is significantly involved in the inhibition of cardiac fibrosis in female mice [68]. The increased angiogenesis/lymphangiogenesis and attenuated fibrosis in female ERα-OE mice following MI could be one explanation for the phenomenon that hearts of female ERα-OE mice did not exhibit accelerated or adverse post-infarct remodelling, indicated by maintained systolic and diastolic volumes and LV wall thickness after MI. However, in male ERα-OE mice, despite the higher angiogenesis/lymphangiogenesis, the activation of JNK-pathway and attenuation of fibrosis were not as pronounced as in female ERα-OE mice post MI. It seems that in male ERα-OE mice the activation of angiogenesis/lymphangiogenesis alone is not sufficient to contribute to the improved remodeling.

Overall, our data suggests that cardiomyocyte-specific ERα provides cardioprotection in female mice by enhancing vascular structure and function, and attenuation of cardiac remodeling in a paracrine fashion in response to cardiac ischemic injury.

Supplementary Material

Refer to Web version on PubMed Central for supplementary material.

Acknowledgments

We thank Arne Kuehne, Britta Fielitz and Petra Domaing for excellent technical support. This work was supported by the Deutsche For schungsgemeinschaft (GRK 754, FOR1054 to VRZ and SM); the German Center for Cardiovascular Research (DZHK) to VRZ; and National Cancer Institute (NIH grants RO1 CA112176 and P30 CA051008 (Animal Shared Resource) to PAF.

Abbreviations

CD31	Platelet/endothelial cell adhesion molecule-1 (Pecam-1)
Col I, Col III	Collagen type I and III
CVD	Cardiovascular Diseases
E2	17β-estradiol, Estrogen
ERα	Estrogen receptor alpha (*Esr1*)
ERα-OE	Cardiomyocyte-specific Overexpression of ERα
GAPDH	Glyceraldehyde 3-Phosphate Dehydrogenase
H&E staining	Hematoxylin-Eosin staining
Hprt	Hypoxanthine Phosphoribosyltransferase
JNK	Mitogen-activated protein kinase c-jun N-terminal Kinase JNK1/3
LAD	Left Anterior Descending coronary artery

LV	Left Ventricle
LVM/TL	LV Mass to Tibia Length
Lyve-1	Lymphatic vessel endothelial hyaluronan receptor-1
MH	Myocardial Hypertrophy
MI	Myocardial Infarction
Myh6, Myh7	Myosin heavy chain 6 and 7
Nppa	Atrial natriuretic peptide
Nppb	Brain natriuretic peptide
Vegf	Vascular endothelial growth factor

References

1. Regitz-Zagrosek V. Therapeutic implications of the gender-specific aspects of cardiovascular disease. Nat Rev Drug Discov. 2006; 5:425–438. [PubMed: 16672926]
2. Beer S, Reincke M, Kral M, Lie SZ, Steinhauer S, et al. Susceptibility to cardiac ischemia/reperfusion injury is modulated by chronic estrogen status. J Cardiovasc Pharmacol. 2002; 40:420–428. [PubMed: 12198328]
3. Shlipak MG, Angeja BG, Go AS, Frederick PD, Canto JG, et al. Hormone therapy and in-hospital survival after myocardial infarction in postmenopausal women. Circulation. 2001; 104:2300–2304. [PubMed: 11696469]
4. Xu Y, Armstrong SJ, Arenas IA, Pehowich DJ, Davidge ST. Cardioprotection by chronic estrogen or superoxide dismutase mimetic treatment in the aged female rat. Am J Physiol Heart Circ Physiol. 2004; 287:H165–171. [PubMed: 14988070]
5. Hale SL, Birnbaum Y, Kloner RA. beta-Estradiol, but not alpha-estradiol, reduced myocardial necrosis in rabbits after ischemia and reperfusion. Am Heart J. 1996; 132:258–262. [PubMed: 8701884]
6. Kim JK, Pedram A, Razandi M, Levin ER. Estrogen prevents cardiomyocyte apoptosis through inhibition of reactive oxygen species and differential regulation of p38 kinase isoforms. J Biol Chem. 2006; 281:6760–6767. [PubMed: 16407188]
7. Patten RD, Pourati I, Aronovitz MJ, Baur J, Celestin F, et al. 17beta-estradiol reduces cardiomyocyte apoptosis in vivo and in vitro via activation of phospho-inositide-3 kinase/Akt signaling. Circ Res. 2004; 95:692–699. [PubMed: 15345655]
8. Booth EA, Marchesi M, Kilbourne EJ, Lucchesi BR. 17Beta-estradiol as a receptor-mediated cardioprotective agent. J Pharmacol Exp Ther. 2003; 307:395–401. [PubMed: 12893838]
9. Booth EA, Marchesi M, Knittel AK, Kilbourne EJ, Lucchesi BR. The pathway-selective estrogen receptor ligand WAY-169916 reduces infarct size after myocardial ischemia and reperfusion by an estrogen receptor dependent mechanism. J Cardiovasc Pharmacol. 2007; 49:401–407. [PubMed: 17577105]
10. Jeanes HL, Tabor C, Black D, Ederveen A, Gray GA. Oestrogen-mediated cardioprotection following ischaemia and reperfusion is mimicked by an oestrogen receptor (ER)alpha agonist and unaffected by an ER beta antagonist. J Endocrinol. 2008; 197:493–501. [PubMed: 18492815]
11. Kolodgie FD, Farb A, Litovsky SH, Narula J, Jeffers LA, et al. Myocardial protection of contractile function after global ischemia by physiologic estrogen replacement in the ovariectomized rat. J Mol Cell Cardiol. 1997; 29:2403–2414. [PubMed: 9299364]
12. Lee TM, Lin MS, Chou TF, Tsai CH, Chang NC. Adjunctive 17beta-estradiol administration reduces infarct size by altered expression of canine myocardial connexin43 protein. Cardiovasc Res. 2004; 63:109–117. [PubMed: 15194467]

13. Nikolic I, Liu D, Bell JA, Collins J, Steenbergen C, et al. Treatment with an estrogen receptor-beta-selective agonist is cardioprotective. J Mol Cell Cardiol. 2007; 42:769–780. [PubMed: 17362982]
14. Squadrito F, Altavilla D, Squadrito G, Campo GM, Arlotta M, et al. 17Beta-oestradiol reduces cardiac leukocyte accumulation in myocardial ischaemia reperfusion injury in rat. Eur J Pharmacol. 1997; 335:185–192. [PubMed: 9369372]
15. Mendelsohn ME, Karas RH. Molecular and cellular basis of cardiovascular gender differences. Science. 2005; 308:1583–1587. [PubMed: 15947175]
16. Grohé C, Kahlert S, Löbbert K, Stimpel M, Karas RH, et al. Cardiac myocytes and fibroblasts contain functional estrogen receptors. FEBS Lett. 1997; 416:107–112. [PubMed: 9369244]
17. Mahmoodzadeh S, Dworatzek E, Fritschka S, Pham TH, Regitz-Zagrosek V. 17beta-Estradiol inhibits matrix metalloproteinase-2 transcription via MAP kinase in fibroblasts. Cardiovasc Res. 2010; 85:719–728. [PubMed: 19861308]
18. Mahmoodzadeh S, Eder S, Nordmeyer J, Ehler E, Huber O, et al. Estrogen receptor alpha up-regulation and redistribution in human heart failure. FASEB J. 2006; 20:926–934. [PubMed: 16675850]
19. Nordmeyer J, Eder S, Mahmoodzadeh S, Martus P, Fielitz J, et al. Upregulation of myocardial estrogen receptors in human aortic stenosis. Circulation. 2004; 110:3270–3275. [PubMed: 15533858]
20. Ropero AB, Eghbali M, Minosyan TY, Tang G, Toro L, et al. Heart estrogen receptor alpha: distinct membrane and nuclear distribution patterns and regulation by estrogen. J Mol Cell Cardiol. 2006; 41:496–510. [PubMed: 16876190]
21. Losordo DW, Kearney M, Kim EA, Jekanowski J, Isner JM. Variable expression of the estrogen receptor in normal and atherosclerotic coronary arteries of premenopausal women. Circulation. 1994; 89:1501–1510. [PubMed: 8149515]
22. Post WS, Goldschmidt-Clermont PJ, Wilhide CC, Heldman AW, Sussman MS, et al. Methylation of the estrogen receptor gene is associated with aging and atherosclerosis in the cardiovascular system. Cardiovasc Res. 1999; 43:985–991. [PubMed: 10615426]
23. Wang M, Crisostomo P, Wairiuko GM, Meldrum DR. Estrogen receptor-alpha mediates acute myocardial protection in females. Am J Physiol Heart Circ Physiol. 2006; 290:H2204–2209. [PubMed: 16415070]
24. Zhai P, Eurell TE, Cooke PS, Lubahn DB, Gross DR. Myocardial ischemia-reperfusion injury in estrogen receptor-alpha knockout and wild-type mice. Am J Physiol Heart Circ Physiol. 2000; 278:H1640–1647. [PubMed: 10775144]
25. Booth EA, Obeid NR, Lucchesi BR. Activation of estrogen receptor-alpha protects the in vivo rabbit heart from ischemia-reperfusion injury. Am J Physiol Heart Circ Physiol. 2005; 289:H2039–2047. [PubMed: 15994857]
26. Novotny JL, Simpson AM, Tomicek NJ, Lancaster TS, Korzick DH. Rapid estrogen receptor-alpha activation improves ischemic tolerance in aged female rats through a novel protein kinase C epsilon-dependent mechanism. Endocrinology. 2009; 150:889–896. [PubMed: 19176323]
27. Vornehm ND, Wang M, Abarbanell A, Herrmann J, Weil B, et al. Acute postischemic treatment with estrogen receptor-alpha agonist or estrogen receptor-beta agonist improves myocardial recovery. Surgery. 2009; 146:145–154. [PubMed: 19628068]
28. Takemura G, Fujiwara H. Role of apoptosis in remodeling after myocardial infarction. Pharmacol Ther. 2004; 104:1–16. [PubMed: 15500905]
29. Kanno S, Lerner DL, Schuessler RB, Betsuyaku T, Yamada KA, et al. Echocardiographic evaluation of ventricular remodeling in a mouse model of myocardial infarction. J Am Soc Echocardiogr. 2002; 15:601–609. [PubMed: 12050601]
30. Petzhold D, Lossie J, Keller S, Werner S, Haase H, et al. Human essential myosin light chain isoforms revealed distinct myosin binding, sarcomeric sorting, and inotropic activity. Cardiovasc Res. 2011; 90:513–520. [PubMed: 21262909]
31. Witt H, Schubert C, Jaekel J, Fliegner D, Penkalla A, et al. Sex-specific pathways in early cardiac response to pressure overload in mice. J Mol Med (Berl). 2008; 86:1013–1024. [PubMed: 18665344]

32. Uchida C, Gee E, Ispanovic E, Haas TL. JNK as a positive regulator of angiogenic potential in endothelial cells. Cell Biol Int. 2008; 32:769–776. [PubMed: 18455449]
33. Wu G, Luo J, Rana JS, Laham R, Sellke FW, et al. Involvement of COX-2 in VEGF-induced angiogenesis via P38 and JNK pathways in vascular endothelial cells. Cardiovasc Res. 2006; 69:512–519. [PubMed: 16336951]
34. Dorn GW 2nd. The fuzzy logic of physiological cardiac hypertrophy. Hypertension. 2007; 49:962–970. [PubMed: 17389260]
35. Eghbali M, Deva R, Alioua A, Minosyan TY, Ruan H, et al. Molecular and functional signature of heart hypertrophy during pregnancy. Circ Res. 2005; 96:1208–1216. [PubMed: 15905459]
36. Fernandes T, Soci UP, Oliveira EM. Eccentric and concentric cardiac hypertrophy induced by exercise training: microRNAs and molecular determinants. Braz J Med Biol Res. 2011; 44:836–847. [PubMed: 21881810]
37. Zhang Y, Novak K, Kaufman S. Atrial natriuretic factor release during pregnancy in rats. J Physiol. 1995; 488:509–514. [PubMed: 8568689]
38. Lannigan DA. Estrogen receptor phosphorylation. Steroids. 2003; 68:1–9. [PubMed: 12475718]
39. Mahmoodzadeh S, Pham TH, Kuehne A, Fielitz B, Dworatzek E, et al. 17β-Estradiol-induced interaction of ERÎ± with NPPA regulates gene expression in cardiomyocytes. Cardiovasc Res. 2012; 96:411–421. [PubMed: 22962310]
40. Ellmers LJ, Knowles JW, Kim HS, Smithies O, Maeda N, et al. Ventricular expression of natriuretic peptides in Npr1(-/-) mice with cardiac hypertrophy and fibrosis. Am J Physiol Heart Circ Physiol. 2002; 283:H707–714. [PubMed: 12124219]
41. Holtwick R, van Eickels M, Skryabin BV, Baba HA, Bubikat A, et al. Pressure-independent cardiac hypertrophy in mice with cardiomyocyte-restricted inactivation of the atrial natriuretic peptide receptor guanylyl cyclase-A. J Clin Invest. 2003; 111:1399–1407. [PubMed: 12727932]
42. Molkentin JD, Dorn GW 2nd. Cytoplasmic signaling pathways that regulate cardiac hypertrophy. Annu Rev Physiol. 2001; 63:391–426. [PubMed: 11181961]
43. Wagner N, Jehl-Piétri C, Lopez P, Murdaca J, Giordano C, et al. Peroxisome proliferator-activated receptor beta stimulation induces rapid cardiac growth and angiogenesis via direct activation of calcineurin. Cardiovasc Res. 2009; 83:61–71. [PubMed: 19351742]
44. Jesmin S, Sakuma I, Hattori Y, Kitabatake A. In vivo estrogen manipulations on coronary capillary network and angiogenic molecule expression in middle-aged female rats. Arterioscler Thromb Vasc Biol. 2002; 22:1591–1597. [PubMed: 12377735]
45. Losordo DW, Isner JM. Estrogen and angiogenesis: A review. Arterioscler Thromb Vasc Biol. 2001; 21:6–12. [PubMed: 11145928]
46. Miller VM, Duckles SP. Vascular actions of estrogens: functional implications. Pharmacol Rev. 2008; 60:210–241. [PubMed: 18579753]
47. Morales DE, McGowan KA, Grant DS, Maheshwari S, Bhartiya D, et al. Estrogen promotes angiogenic activity in human umbilical vein endothelial cells in vitro and in a murine model. Circulation. 1995; 91:755–763. [PubMed: 7530174]
48. Urbich C, Dimmeler S. Risk factors for coronary artery disease, circulating endothelial progenitor cells, and the role of HMG-CoA reductase inhibitors. Kidney Int. 2005; 67:1672–1676. [PubMed: 15840010]
49. Ardelt AA, McCullough LD, Korach KS, Wang MM, Munzenmaier DH, et al. Estradiol regulates angiopoietin-1 mRNA expression through estrogen receptor-alpha in a rodent experimental stroke model. Stroke. 2005; 36:337–341. [PubMed: 15637314]
50. Brouchet L, Krust A, Dupont S, Chambon P, Bayard F, et al. Estradiol accelerates reendothelialization in mouse carotid artery through estrogen receptor-alpha but not estrogen receptor-beta. Circulation. 2001; 103:423–428. [PubMed: 11157695]
51. Johns A, Freay AD, Fraser W, Korach KS, Rubanyi GM. Disruption of estrogen receptor gene prevents 17 beta estradiol-induced angiogenesis in transgenic mice. Endocrinology. 1996; 137:4511–4513. [PubMed: 8828515]
52. Pare G, Krust A, Karas RH, Dupont S, Aronovitz M, et al. Estrogen receptor-alpha mediates the protective effects of estrogen against vascular injury. Circ Res. 2002; 90:1087–1092. [PubMed: 12039798]

53. Gagliardi A, Collins DC. Inhibition of angiogenesis by antiestrogens. Cancer Res. 1993; 53:533–535. [PubMed: 7678775]
54. Zaitseva M, Yue DS, Katzenellenbogen JA, Rogers PA, Gargett CE. Estrogen receptor-alpha agonists promote angiogenesis in human myometrial microvascular endothelial cells. J Soc Gynecol Investig. 2004; 11:529–535.
55. Banai S, Shweiki D, Pinson A, Chandra M, Lazarovici G, et al. Upregulation of vascular endothelial growth factor expression induced by myocardial ischaemia: implications for coronary angiogenesis. Cardiovasc Res. 1994; 28:1176–1179. [PubMed: 7525061]
56. Hoeben A, Landuyt B, Highley MS, Wildiers H, Van Oosterom AT, et al. Vascular endothelial growth factor and angiogenesis. Pharmacol Rev. 2004; 56:549–580. [PubMed: 15602010]
57. Ishikawa Y, Akishima-Fukasawa Y, Ito K, Akasaka Y, Tanaka M, et al. Lymphangiogenesis in myocardial remodelling after infarction. Histopathology. 2007; 51:345–353. [PubMed: 17727476]
58. Buteau-Lozano H, Ancelin M, Lardeux B, Milanini J, Perrot-Applanat M. Transcriptional regulation of vascular endothelial growth factor by estradiol and tamoxifen in breast cancer cells: a complex interplay between estrogen receptors alpha and beta. Cancer Res. 2002; 62:4977–4984. [PubMed: 12208749]
59. Gargett CE, Zaitseva M, Bucak K, Chu S, Fuller PJ, et al. 17Beta-estradiol up-regulates vascular endothelial growth factor receptor-2 expression in human myometrial microvascular endothelial cells: role of estrogen receptor-alpha and -beta. J Clin Endocrinol Metab. 2002; 87:4341–4349. [PubMed: 12213896]
60. Hamada H, Kim MK, Iwakura A, Ii M, Thorne T, et al. Estrogen receptors alpha and beta mediate contribution of bone marrow-derived endothelial progenitor cells to functional recovery after myocardial infarction. Circulation. 2006; 114:2261–2270. [PubMed: 17088460]
61. Jesmin S, Mowa CN, Sultana SN, Shimojo N, Togashi H, et al. VEGF signaling is disrupted in the hearts of mice lacking estrogen receptor alpha. Eur J Pharmacol. 2010; 641:168–178. [PubMed: 20639141]
62. Sengupta K, Banerjee S, Saxena NK, Banerjee SK. Thombospondin-1 disrupts estrogen-induced endothelial cell proliferation and migration and its expression is suppressed by estradiol. Mol Cancer Res. 2004; 2:150–158. [PubMed: 15037654]
63. Cochain C, Channon KM, Silvestre JS. Angiogenesis in the infarcted myocardium. Antioxid Redox Signal. 2013; 18:1100–1113. [PubMed: 22870932]
64. Cui Y. The role of lymphatic vessels in the heart. Pathophysiology. 2010; 17:307–314. [PubMed: 19942415]
65. Laine GA, Allen SJ. Left ventricular myocardial edema. Lymph flow, interstitial fibrosis, and cardiac function. Circ Res. 1991; 68:1713–1721. [PubMed: 2036720]
66. Park JH, Yoon JY, Ko SM, Jin SA, Kim JH, et al. Endothelial progenitor cell transplantation decreases lymphangiogenesis and adverse myocardial remodeling in a mouse model of acute myocardial infarction. Exp Mol Med. 2011; 43:479–485. [PubMed: 21694495]
67. Davis KL, Laine GA, Geissler HJ, Mehlhorn U, Brennan M, et al. Effects of myocardial edema on the development of myocardial interstitial fibrosis. Microcirculation. 2000; 7:269–280. [PubMed: 10963632]
68. Westphal C, Schubert C, Prelle K, Penkalla A, Fliegner D, et al. Effects of estrogen, an ERα agonist and raloxifene on pressure overload induced cardiac hypertrophy. PLoS One. 2012; 7:e50802. [PubMed: 23227210]

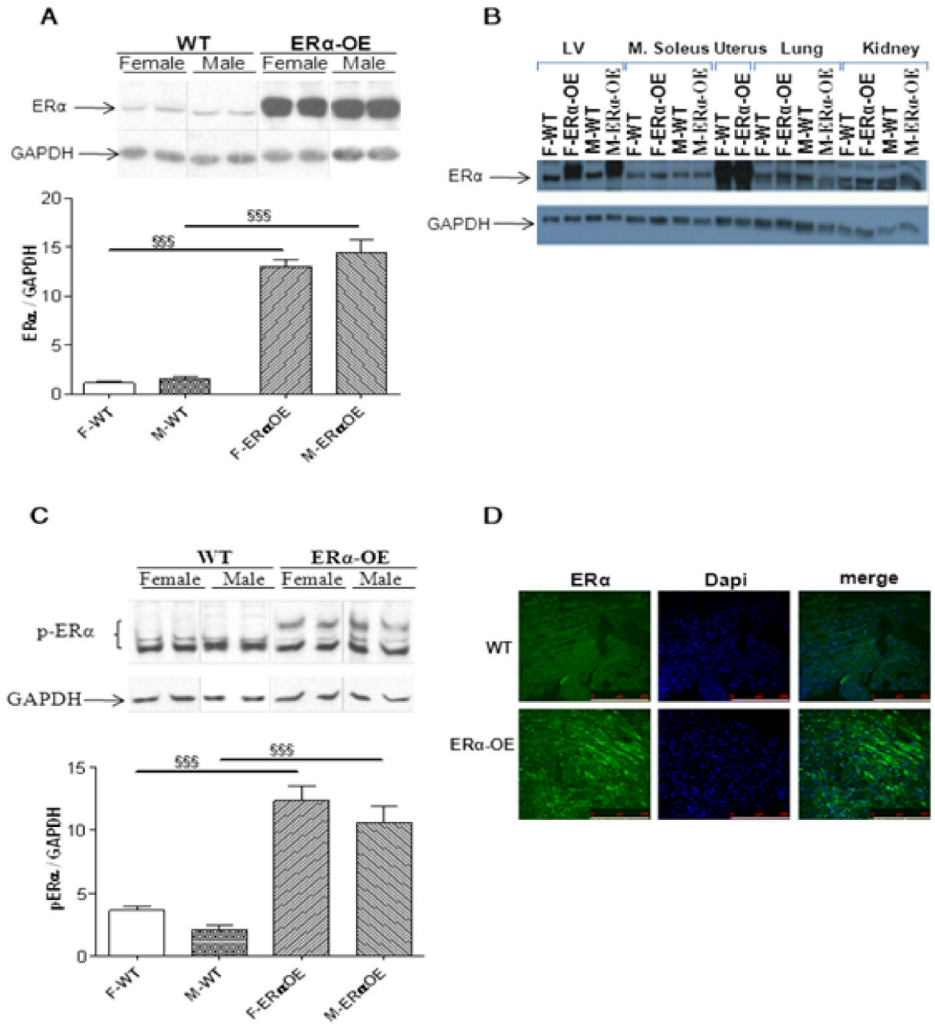

Figure 1.

Characterization of ERα-OE mice (**A-C**): Representative Western blots demonstrate that **A**: ERα levels are significantly higher in the LV tissue of female and male ERα-OE mice compared to WT-mice, **B**: ERα protein is overexpressed only in the LV tissue, but not in soleus muscle, uterus, lung and kidney of ERα-OE mice. Uterus was used as positive control. **C**: The phosphorylation level of ERα at Serin-118 is significantly higher in the LV of both female and male ERα-OE mice compared to those in WT-mice. GAPDH was used as loading control protein for Western blot analysis and protein normalization. ERα/GAPDH and pERα/GAPDH ratios are indicated below each Western blot (A&C). Each bar represents the mean ± SEM (n=7-10 mice per each group). § for the genotype effect (ERα-OE vs. WT, $p<0.001$). **D**: Immunofluorescence analysis followed by confocal laser microscopy of 3μm paraffin sections revealed higher expression and more intense nuclear localization of transgenic ERα (green) in the cardiomyocytes of ERα-OE mice. Nuclei are shown in blue (Dapi). 20× magnification, scale bar 250μm.

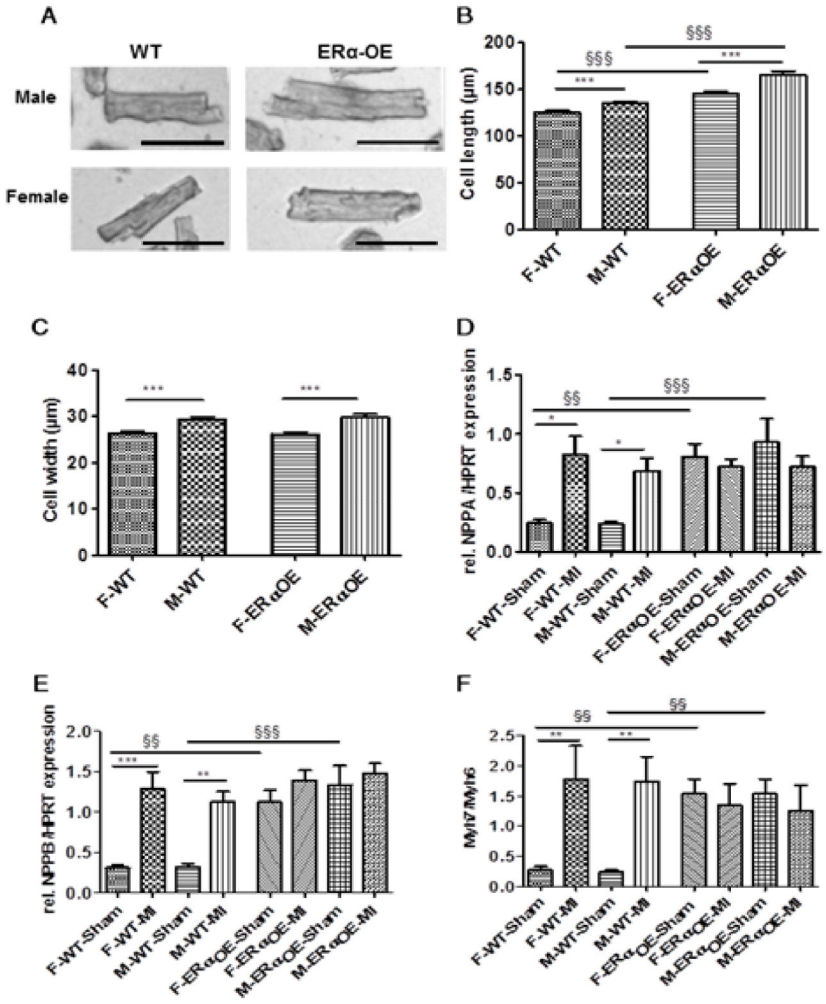

Figure 2.

ERα-overexpression promotes cardiac hypertrophy in the basal state in both sexes. **A**: Representative micrographs of single cardiomyocytes of WT- and ERα-OE mice (40× magnification, scale bar 100μm). **B-C**: Quantification of diastolic cell length and cardiomyocytes width. Compared to WT, cardiomyocytes isolated from female and male ERα-OE displayed a significant increase in diastolic cell length, but no changes in cell width at the basal level. Data are given as mean ± SEM for 100 to 300 cells per group. § for the genotype effect (ERα-OE vs. WT, $p<0.001$); * for females vs. males ($p<0.001$). **D-F**: Expression analysis of hypertrophy markers. **D**: *Nppa*, **E**:*Nppb*, and **F**: the ratio of *Myh7/ Myh6* expression in the LV tissues of female and male ERα-OE mice compared with WT-mice. §for the genotype effect (ERα-OE vs. WT, females: $p<0.01$, $p<0.01$, $p<0.01$; males: $p<0.001$, $p<0.001$, $p<0.01$, for each gene). * for MI effect (MI vs. sham, females: $p<0.05$, $p<0.001$, $p<0.01$, males: $p<0.05$, $p<0.01$, p0.01,for each gene). $n\geq10$.

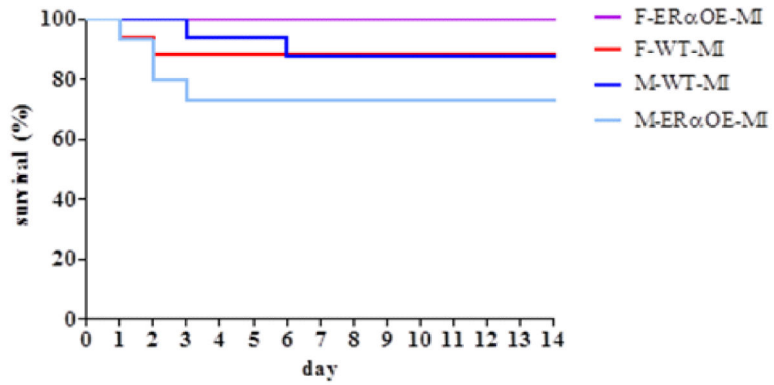

Figure 3.

Comparison of survival curves from female and male ERα-OE and WT mice 2 weeks after MI. In comparison to the other groups, only the female ERα-OE mice survived 100% after the acute phase (without first 24h; n=13-17 per group), however this difference was not statistically significant (p=0.209 vs. female WT, by log-rank test).

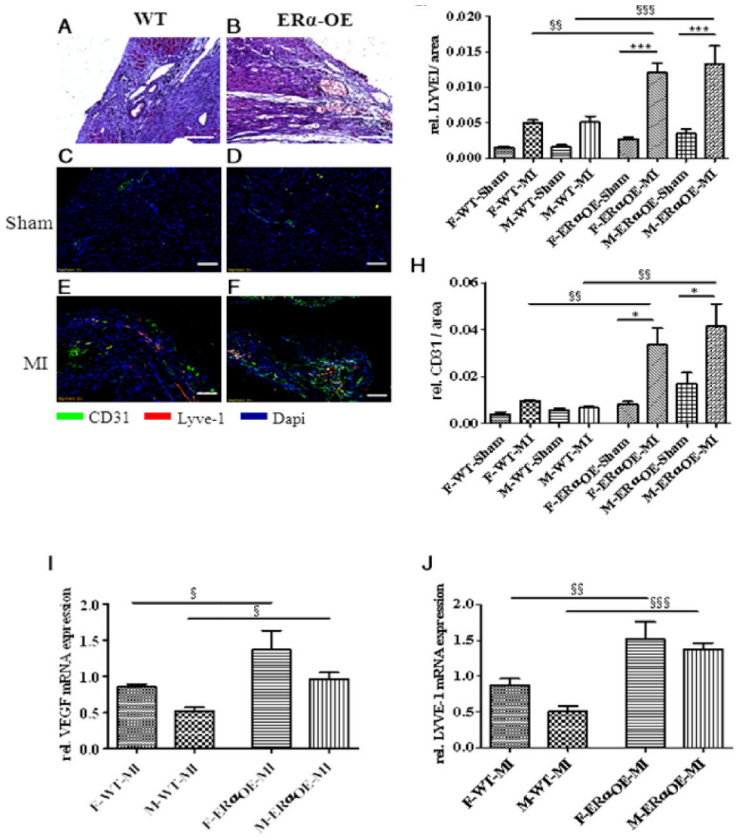

Figure 4.

ERα-overexpression in cardiomyocytes accelerates both angiogenesis and lymphangiogenesis predominantly in the peri-infarct areas in both sexes. **A-B**: Representative images of H&E-stained paraffin sections of LV tissues from WT- and ERα-OE mice after MI. ERα-OE mice hearts showed an increased occurrence of vascular-like structures in the peri-infarct area. 20× magnification, scale bar 100μm. **C-F**: Representative immunofluorescence photographs of LV tissues 2 weeks after sham and MI operationfrom WT-(C **and E**) and ERα-OE (**D and F**) mice with CD31 and LYVE-1staining (scale bar 100 μm). For a better illustration of CD31 and LYVE-1 signals, higher magnification of the LV areas with strongest signals, i.e. in the peri-infarct area, have been shown. CD31-positive vessels (green), LYVE-1 positive vessels (red), nuclei (DAPI,blue).**G-H**:Quantification of areas of LYVE-1 and CD31 expressing vessels fromwhole LV cross-sectional areas.Data expressed as mean ± SEM of 3 to 4 animals per group. § for the genotype effect: females: p<0.01 (LYVE-1), p<0.01 (CD31); males: p<0.001 (LYVE-1), p<0.01 (CD31). *for MI effect: females: p<0.001 (LYVE-1), p<0.05 (CD31); males: p<0.001 (LYVE-1), p<0.05 (CD31). **I-J**: qRT-PCR analysis of the mRNA levels of *Vegf* and *Lyve*-1 in the peri-infarct and infarct areas from WT- and ERα-OE mice. Data expressed as mean ± SEM of 5 to 6 animals per group. § for the genotype effect for each gene: females: p<0.05(*Vegf*) and p<0.01 (*Lyve*-1); males: p<0.05(*Vegf*) and 0.001 (*Lyve*-1).

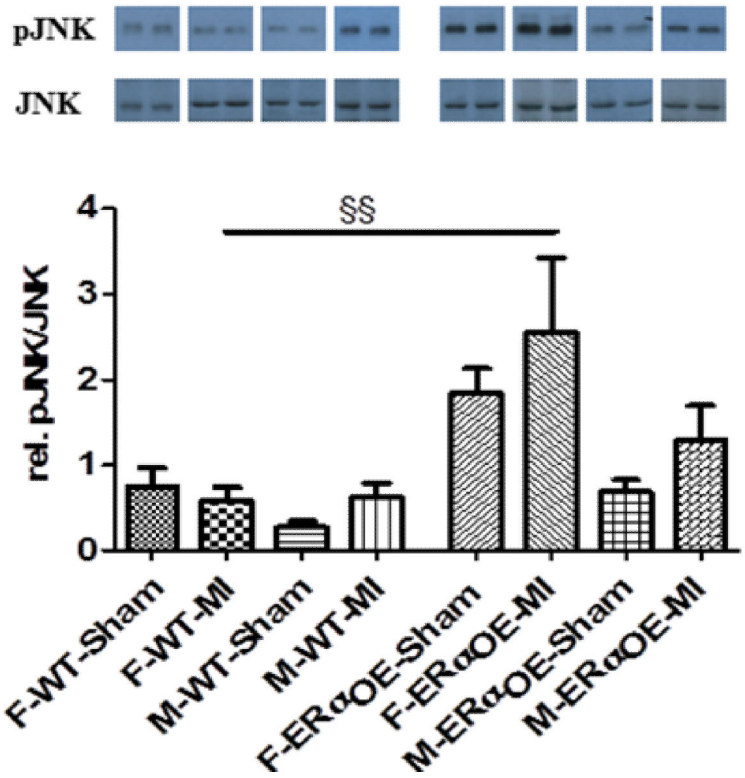

Figure 5.

Phosphorylation level of JNK (pJNK) is increased in only female ERα-OE mice hearts. Representative Western blots (top) and bar graph(bottom) representing the quantitative Western blot analysis of pJNK in LV tissues from female and male WT and ERα-OE mice. Data are expressed as ratio of pJNK to JNK expression. Bars represent the mean ± SEM of 7 to 8 animals per group. § for genotype effect: $p<0.01$.

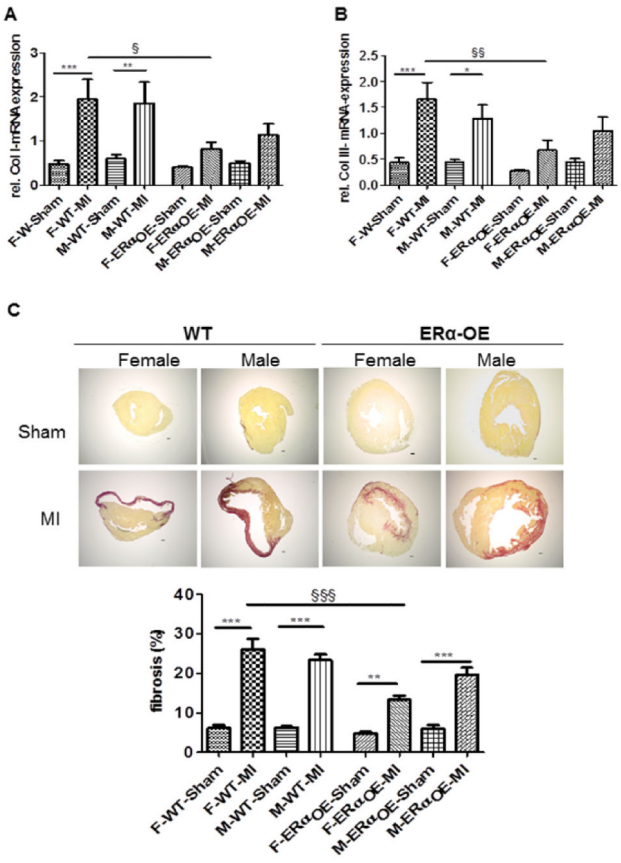

Figure 6.

Cardiomyocyte-specific overexpression of ERα attenuates fibrosis**. A-B**: Assessment of mRNA expression of fibrosis markers *Col* I and III in the LV tissues from female and male WT- and ERα-OE mice 2 weeks after sham and MI by qRT-PCR. ERα-OE attenuates the MI-induced expression of *Col* I and III after MI. Data expressed as mean ±SEM; n ≥ 8 mice per group. § for the genotype effect: females: $p<0.05$ and $p<0.01$ for each gene. *for MI effect for each gene: WT-female: $p<0.001$; ERα-OE-female: $p<0.001$;WT-male: $p<0.01$ and ERα-OE-male $p<0.05$. **C**: Sirius red staining of representative LV tissue (upper panel, scale bar 200 μm) and fibrosis quantification expressed as the percent of fibrosis area in entire LV cross-section (lower panel) in WT- and ERα-OE mice 2 weeks after sham or MI surgery. The extent of interstitial collagen accumulation in female ERα-OE was significantly less in comparison to female WT-mice after MI. Data expressed as mean ± SEM of 4 to 6 animals per group. § for the genotype effect: $p<0.001$. * for MI effect (MI vs. sham): WT-female: $p<0.001$ and ERα-OE-female $p<0.01$; WT-male: $p<0.001$ and ERα-OE.

Table 1

Morphological and echocardiography parameters 2 weeks after sham and MI surgery in female and male WT- and ERα-OE mice.

Genotype	**WT-mice**				**ERα-OE mice**			
Sex	**Female**		**Male**		**Female**		**Male**	
Treatment	**Sham (n=12)**	**MI (n=11)**	**Sham (n=18)**	**MI (n=12)**	**Sham (n=14)**	**MI (n=9)**	**Sham (n=15)**	**MI (n=9)**
BW [g]	22.03 ± 0.52	21.48 ± 0.54	28.17 ± 0.60	28.58 ± 0.78	22.33 ± 0.52	21.31 ± 0.53	27.64 ± 0.57	27.53 ± 0.75
TL [mm]	16.32 ± 0.13	16.35 ± 0.16	16.86 ± 0.09	16.81 ± 0.16	16.66 ± 0.11	16.39 ± 0.13	16.91 ± 0.10	16.54 ± 0.16
LVM [mg]	84.69 ± 2.97	90.94 ± 1.99	113.97 ± 2.10	121.10 ± 4.31	103.66§ ± 3.22	105.93 ± 4.07	134.98§ ± 5.91	130.90 ± 4.27
LVM/TL [mg/mm]	5.19 ± 0.17	5.57 ± 0.14	6.76 ± 0.13	7.20 ± 0.24	6.23§ ± 0.20	6.46 ± 0.24	7.98§ ± 0.34	7.90 ± 0.23
LVW [mm]	0.63 ± 0.02	0.57* ± 0.01	0.71 ± 0.01	0.62* ± 0.01	0.64 ± 0.01	0.62 ± 0.02	0.73 ± 0.01	0.65* ± 0.02
LVVol,d [μl]	40.90 ± 1.81	67.43* ± 6.64	52.71 ± 2.14	95.77* ± 8.95	59.75§ ± 3.25	74.64 ± 4.76	63.56§ ± 3.52	94.53* ± 5.32
LVVol,s [μl]	14.01 ± 1.26	47.51* ± 6.14	19.98 ± 1,18	67.74* ± 10.72	31.23§ ± 3.24	50.50 ± 6.30	31.63§ ± 2.93	69.40* ± 5.55
HR [bpm]	480.3 ± 14.80	525.5 ± 12.36	495.8 ± 10.12	515.8 ± 12.65	472.5 ± 11.66	459.6 ± 20.26	462.5 ± 20.21	522.3 ± 38.54
LVSV [μl]	26.89 ± 1.31	19.92 ± 1.28	32.73 ± 1.28	28.03 ± 2.35	28.52 ± 1.65	24.14 ± 2.53	31.45 ± 1.90	24.65 ± 3.03
LVCO [ml/min]	13.11 ± 0.86	10.41 ± 0.64	16.16 ± 0.71	14.72 ± 1.39	13.49 ± 1.01	10.25 ± 1.19	15.33 ± 1.13	12.42 ± 1.32
Infarctsize (%)	—	35.23 ± 3.38	—	33.46 ± 3.92	—	29.18 ± 3.28	—	28.89 ± 3.61

Data are means ± SEM. MI: Myocardial Infarction; Sham: sham operation; F: female; M: male; n: number of animals; BW: body weight; TL: tibia length; HW: heart weight; LVM: left ventricular (LV) mass; LVW: LV wall thickness; LVVol,d: LV diastolic volume; LVVol,s: LV systolic volume; HR: heart rate; LVSV: LV stroke volume; LVCO: LV cardiac output. All data are shown as Mean ± SEM.

* $p<0.05$ MI vs. sham,

§ $p<0.05$ ERa-OE vs. WT